OxiTidy v.1: Motion Artifact Detection in Photoplethysmographic Signals Using Artificial Neural Network. ⋆

Caíque Santos Lima * **Rafael Vidal Aroca** **
André Carmona Hernandes ***

* *Department of Electrical Engineering, Federal University of São Carlos, SP (e-mail: ccaique.lima@gmail.com)*
** *Computing Department, Federal University of São Carlos, SP (e-mail: aroca@ufscar.br)*
*** *Department of Electrical Engineering, Federal University of São Carlos, SP (e-mail: andre.hernandes@ufscar.br)*

Abstract:
Pulse oximetry is a non-invasive technique that allows the monitoring of physiological parameters in a very simplified way from photoplethysmographic (PPG) signals. What was possible to do only with high-cost and unwieldy biomedical equipment, has been popularized with the emergence of wearable devices. However, the way these devices are built and used directly influences the quality of the information provided to the user. PPG signals are susceptible to noise, which is largely caused by user movement during monitoring. This can cause errors in the readings and false alarms. In order to mitigate these undesirable effects, this paper proposes an algorithm called OxiTidy v.1 based on artifical neural network (ANN) capable of detecting noise in the PPG signals. These affected samples were not used to the measurements computation, instead a linear interpolation between two normal measurements of oxygen saturation (SpO_2) or heart rate (HR) was performed. The algorithms proposed in this work were tested in the prototype of a Wi-Fi pulse oximeter developed at the Federal University of São Carlos (UFSCar). The results indicated that an ANN (3-3-1) based on multilayer perceptron (MLP) was able to improve SpO_2 and HR estimations both at rest and in motion. OxiTidy v.1 identified the intervals where the measurements were incorrect and then interpolated new values with a good approximation to the readings performed by a pulse oximeter certified by Anvisa.

Keywords: Photoplethysmography; motion artifact detection; machine learning; multilayer perceptron; signal processing; oxygen saturation; heart rate; pulse oximeter; wearables.

1. INTRODUCTION

Lately, wireless biomedical vital signs sensors have gained space in domestic use and are no longer exclusive to large hospitals and clinics (Rodrigues et al., 2017)(Chacon et al., 2019). These sensors became popular with the emergence of wearable devices, initially developed to track physical activities, now evolving into applications in sports, medicine, studies of people's habits, risk assessment of injuries during physical exercise, monitoring of the elderly, monitoring of physiological signals, among other diverse applications for this promising technology (Haghi et al., 2017).

One of the ways to know the level of oxygen essential for the vital functions of the body is to measure the percentage of oxygen available in the hemoglobins (Hb). This can be done using a pulse oximeter. This device, in addition to indirectly measuring oxygen saturation (SpO_2), also measures heart rate (HR). The measurements performed by pulse oximeters are obtained through the phenomenon of photoplethysmography (PPG). SpO_2 obtained through pulse oximetry is important to evaluate cases of hypoxemia, pulmonary embolism, congenital heart disease, acute heart failure and chronic obstructive pulmonary disease (Sinchai et al., 2018).

Through the photoplethysmographic technique, optical properties of body tissue and blood can be characterized using a photodetector and two light sources: a red (660 nm) and an infrared (940 nm). The intensity of the reflected light changes when the volume of the arterial vessel changes during the systolic phase, which is the ejection phase of blood during the cardiac cycle. This variation in light intensity is converted into an electrical signal by the oximeter. Pulsatile arterial blood absorbs and modulates the light emitted by the LEDs that passes through body tissue and forms the PPG signal. The AC (alternating current) component of this signal, represented by the light absorbed by pulsatile arterial blood, is the only variable term. While the DC (direct current) component, represented by the light absorbed by non-pulsatile arterial blood, venous blood and tissues such as skin, nerves and
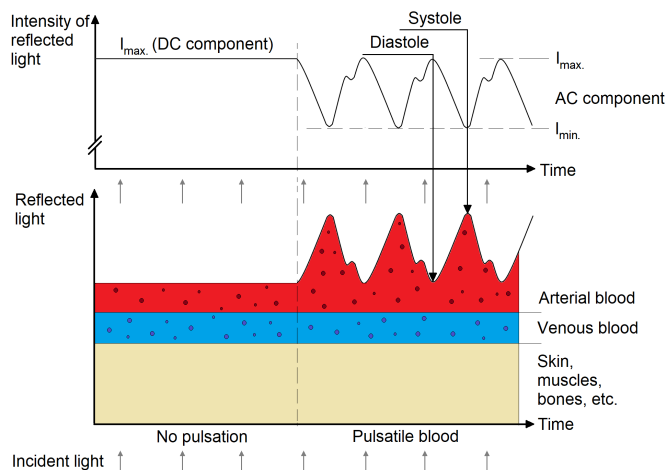
Figure 1. Light reflection during plethysmographic measurement. Adapted from Urpalainen (2011).

bones, remains static (Chacon et al., 2019). Figure 1 shows the components of the PPG signal described above.

It should be noted that the DC and AC components of the generated PPG signals are different for each LED. This is due to the distinct absorption characteristics of Hb, oxyhemoglobin (HbO$_2$) and other body tissue components for different wavelengths. From this difference, it is possible to calculate the oxygen saturation in the blood (Chacon et al., 2019). HR values can be estimated based on the PPG signal as there is a strong influence of cardiac activity on the pulsatile nature of arterial blood flow (Johnston, 2006). It is worth noting that for this, conventionally, only the infrared PPG signal is used, although it is also possible to obtain HR through the red PPG signal.

As will be discussed in subsection 1.2, user motion not only causes a loss of SpO$_2$ and HR measurements, but it can also cause false alarms, displayed warnings of desaturation (hypoxemia) even though the patient is fine. Under certain circumstances this is quite common, a study in the pediatric intensive care unit found that 71% of all pulse oximeter alarms were false (Barker, 2002). This can be very risky, according to Barker (2002, p. 967), "[...] This frequent false-positive rate encourages nurses and other care providers to manually disable alarms, thereby risking failure to detect actual sudden hypoxemia."

Given the importance of correctly obtaining these measurements, in this paper, is proposed a new approach based on artificial neural network (ANN) and inertial measurement unit (IMU) used to detect affected samples of PPG signals and prevent SpO$_2$ and HR measurements from being displayed incorrectly to the user. These affected samples were not used to the measurements computation, instead a linear interpolation between two normal measurements of SpO$_2$ or HR was performed. The fidelity of the results generated by this algorithm was determined by comparing the estimated SpO$_2$ and HR with a reference value measured by a pulse oximeter certified by the Brazilian Health Regulatory Agency (Anvisa).

This paper describes the importance of using the oximeter, its measurement principle (subsection 1.1), issues related to artifact errors (subsection 1.2) and how to treat them (subsection 1.3). The rest of the paper is organized as

follows: section 2 presents the techniques and materials used in this work, section 3 describes how the proposed algorithm works, section 4 discusses the evaluation metrics and algorithms performance, and section 5 concludes the paper.

1.1 Measurement Principle

To get SpO$_2$ from the PPG signals it is necessary to obtain the AC and DC components first. A simple and quick way to do this is to use differentials, as demonstrated by Mendelson (1992). The DC components in this approach can be obtained from the average value of a samples section of the PPG signal, in this same section, the absolute derivative is averaged to produce the AC component. Oxygen saturation can be obtained by calculating the ratio of red and infrared LED lights. The AC and DC components of the PPG signals are normalized (calculating the ratio of AC to DC) to obtain the R ratio, which is given by the ratio of normalized red light to normalized infrared light, according to the following equation:

$$R = \frac{AC_{red}/DC_{red}}{AC_{infrared}/DC_{infrared}}. \tag{1}$$

Finally, SpO$_2$ is calculated from a linear approximation determined by the sensor manufacturer (Maxim Integrated, 2018), where its coefficients are found through empirical data obtained through a calibration process named CO-oximetry. The coefficients presented in equation 2 below were determined by the manufacturer of the PPG sensor used in this work.

$$SpO_2 = 104 - 17 \times R \tag{2}$$

According to the World Health Organization (2011), oxygen saturation in healthy people of any age should be 95% or higher. If a person's SpO$_2$ is 94% or less, they should be evaluated quickly to identify and treat the cause. Levels below 90% are considered a clinical emergency and should be treated urgently.

To estimate HR, the absolute derivative of the PPG signal can be used to identify the pulse peaks, it determines the number of times the heart beats. These peaks are generated in the systolic phase and the interval at which they occur determines the duration of a cardiac cycle (Johnston, 2006). The number of pulse peaks that occur in a 60-second period determines the HR in beats per minute (bpm). According to Johns Hopkins Medicine (2022), the normal pulse rate for healthy adults ranges from 60 to 100 bpm, but it may fluctuate and increase with exercise, illness, injury and emotions.

In this work, the SpO$_2$ and HR measurements obtained through these methods demonstrated above, were named *raw*, i.e., the measurements were only computed and no further processing was done. On the other hand, the new approach propoused in this paper is named *OxiTidy v.1*.

1.2 Artifact Induced Errors

It should be considered that the result of the oximetric reading is influenced by the way the device is used and,

especially, by the quality of the device (Giuliano and Liu, 2006). The accuracy of pulse oximeters tends to decrease as external factors interfere with the PPG signal, i.e., external lights and device movements due to breathing and/or user movement, such as: walking, finger tremors, hand movement, among others (Lee et al., 2003).

According to Hayes and Smith (2001), and Yousefi et al. (2014), the movement in the oximeters is the most common problem of noise in the PPG signal, which can affect it and even corrupt it to the point that it is impossible to use it in the monitoring of SpO_2 and HR. In Figure 2, it is possible to observe that in the range where the oximeter is moving (B), both PPG signals are affected (A). This causes changes in the *raw* SpO_2 (C) and *raw HR* (D) estimations, which drastically reduces the oxygen saturation value displayed in the range where the user's hand is moving. In this interval, readings from static reference oximeter showed SpO_2 remained constant (see *SpO_2 ref.*). Comparing the normal value of the reference with the *raw* estimation of SpO_2, it is possible to observe the false alarm the movement caused.

1.3 Related Work: Artifact Reduction

According to Hayes and Smith (2001), and Lee et al. (2003), removing noise caused by user movement from the PPG signal may not be a simple task when using only signal processing techniques, such as a filter that has a fixed cutoff frequency. Usually, the respiration frequency band is $0.04 - 1.6$ Hz; the pulse wave of the oximeter is $0.5 - 4$ Hz; and the frequency band of noise caused by user movement is 0.1 Hz or more. Therefore, it is complex to remove the noise, since its frequency band is superimposed on the user's pulse wave measured by the oximeter (Lee et al., 2003).

Since motion noise is a problem, several techniques have been used to detect and remove it. Among them, moving average is a method that can be used to eliminate noise, although for cases where the patient has continuous chills and recurrent tremors, the SpO_2 error can be considerably large (Lee et al., 2003). Another approach to dealing with noise is adaptive filters, in addition to being easy to implement, they can also be used in real-time applications, but their main disadvantage is that to provide the input signals it is necessary to install additional sensors (Salehizadeh et al., 2014).

Digital signal processing (DSP) techniques can also be applied in order to mitigate noise caused by movement. Among them are: the Fast Fourier Transform (FFT) and the Smoothed Pseudo Wigner-Ville Distribution (SP-WVD) (Cho et al., 2014). In addition to the DSP techniques applied for decades, other mechanisms can also be applied with the same objective of improving the performance of pulse oximeters, for example, algorithms based on artificial intelligence for photoplethysmographic wave correction (Barker, 2002)(Tarvirdizadeh et al., 2020). Among the clever techniques that are able to detect noise from movement and reconstruct, in real time, the corrupted parts of the PPG signal, the following stand out: the modeling based on the multilayer perceptron (MLP), radial basis function (RBF) and adaptive neuro-fuzzy inference system (ANFIS).

2. MATERIALS AND METHODS

Aiming to investigate the interferences in the PPG signals caused by the oximeter motion, 40 oximetry records were collected from the author*, each one lasting 72 seconds, using a MAX30102 PPG sensor manufactured by Maxim Integrated. These records were collected over three consecutive days, in the three periods of the day: during the morning, in the afternoon and at night. To record the intensity of the movements applied to the oximeter, an MPU-9250 accelerometer produced by InvenSense Inc. was used.

During each collection, movements were produced in order to affect the PPG signals for half of the total time of 72 seconds, i.e., during the initial 18 seconds, the oximeter was kept at rest, then it was moved for 36 seconds and, for end, returned to be held at rest in the final 18 seconds. This approach was adopted so that there was a balance between the amount of affected and normal samples. To signal these moments, a buzzer was used as a beeper. The data that make up this dataset were sampled at a frequency of 50 Hz. Logged information includes NTP (Network Time Protocol); the time in milliseconds; the strength of the infrared and red PPG signals; the acceleration (acc) on the x, y and z axes; SpO_2 and HR measured by an Anvisa-certified pulse oximeter; and, finally, a column that identifies the samples affected by motion artifacts (MAs), manually labeled from rest and motion times. A Wemos D1 Mini microcontroller was also used, a Wi-Fi board based on ESP-8266EX. The items that make up the oximeter under development [1] are shown in Figure 3.

To compare the SpO_2 and HR values measured by the oximeter under development with a reference value, a pulse oximeter Model L5 (Anvisa registration no. 81334699002) was used. To synchronize these SpO_2 and HR samples obtained by the two oximeters, a camera captured images from the standard oximeter so that it was possible to synchronize them with the samples obtained by the oximeter under development. The idea behind this method was to automate the SpO_2 and HR reading and recording process, eliminating the need to manually take notes, avoiding information loss and data synchronization problems.

It is common when working with digital data the presence of high frequency noise that can affect the signal, for this issue, a digital filter is applied that increases the accuracy of the data without distorting the signal tendency. One of the most commonly used and frequently cited solution is the digital filter presented by Savitzky and Golay (1964), popularly named as Savitzky-Golay filter, or simply *savgol*. Savgol is a type of low-pass filter that derive directly from the time-domain problem of data smoothing, moreover, it has highly desirable properties for this application (Press and Teukolsky, 1990). As demonstrated by Gallagher (2020, p. 1), "[...] for a given signal measured at N points and a filter of width w, savgol calculates a polynomial fit of order o in each filter window as the filter is moved across the signal."

---

[1] This is an open project to assist in remote monitoring of patients by measuring HR, SpO_2 and temperature. This system automatically collects data and sends it to a cloud server, which enables remote monitoring of patients. More information can be accessed on the project website: `https://bipes.net.br/UFSCar/oximetro/`
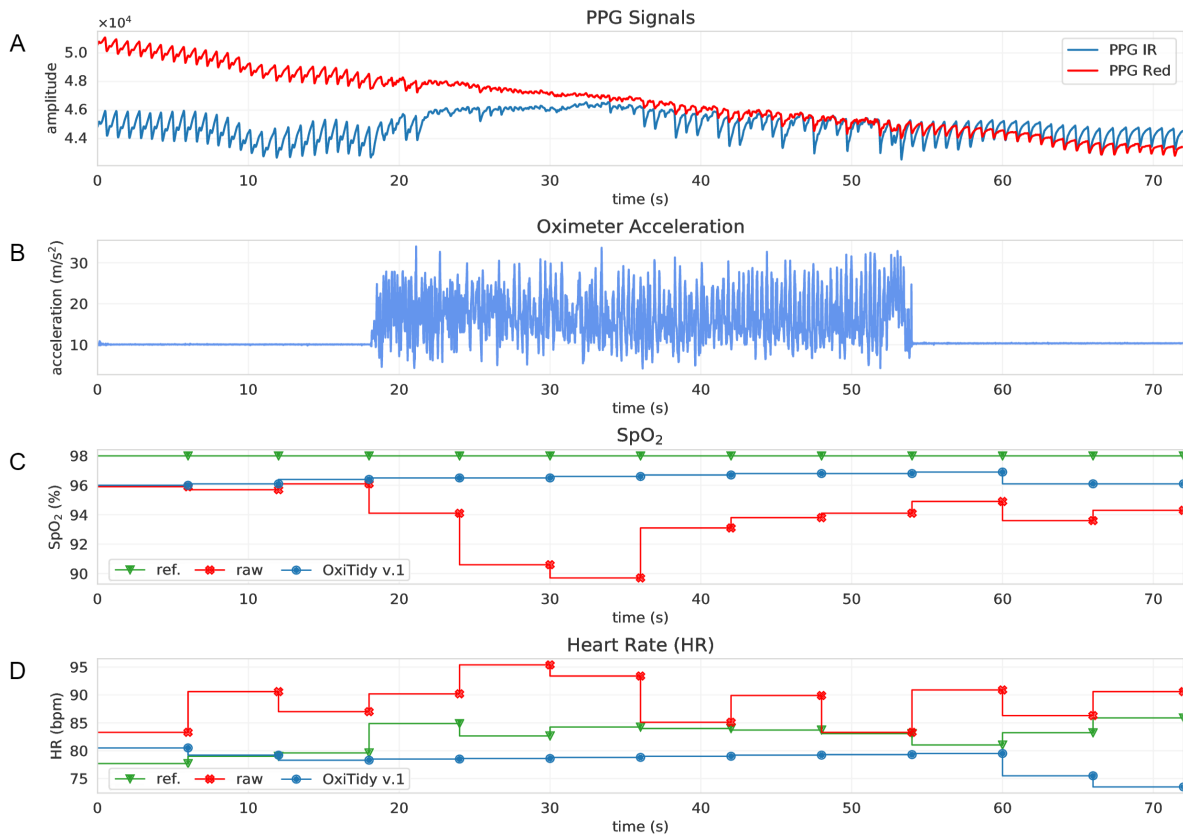
Figure 2. SpO$_2$ and HR affected by motion artifacts. (A) Both PPG signals, infrared (IR) and red, affected in the range where the oximeter moves. (B) Range where the oximeter moves. (C) Effect produced on SpO$_2$ in the range where the oximeter moves. (D) Effect produced on HR in the range where the oximeter moves.
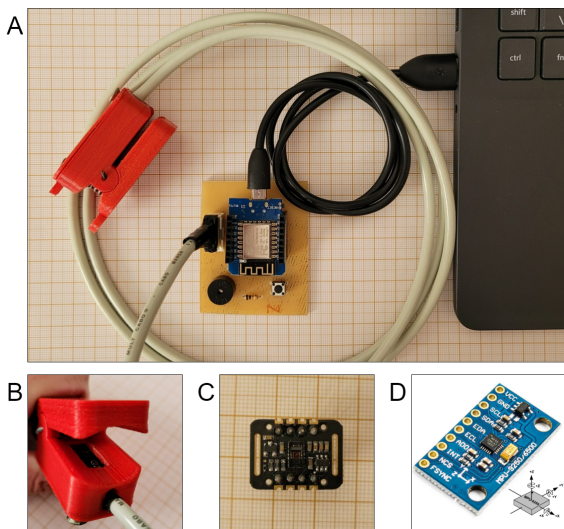
Figure 3. Pulse oximeter components under development. (A) Pulse oximeter kit. (B) Fingertip-clip that houses the sensors. (C) MAX30102 reflective PPG sensor. (D) MPU-9250 3-axis accelerometer, adapted from InvenSense Inc. (2014) and ElectroPeak Inc. (2021).

2.1 Experimental Protocol

The purpose of this experiment was to compare the performance of two different methods (*raw* and *OxiTidy*) in estimating SpO$_2$ and HR while the oximeter was at rest and in motion. To this end, the standard oximeter was placed on the left hand fingertip and kept at rest throughout (72 s). While the developing oximeter was placed on the fingertip of the right hand and during half of the collection time (36 s), random movements were applied in order to affect the PPG signals. Figure 4 depicts how the data were recorded. In order to identify the values recorded by the oximeter certified by Anvisa (left hand), the images captured by the camera were used to analyze the records performed and result SpO$_2$ and HR values.
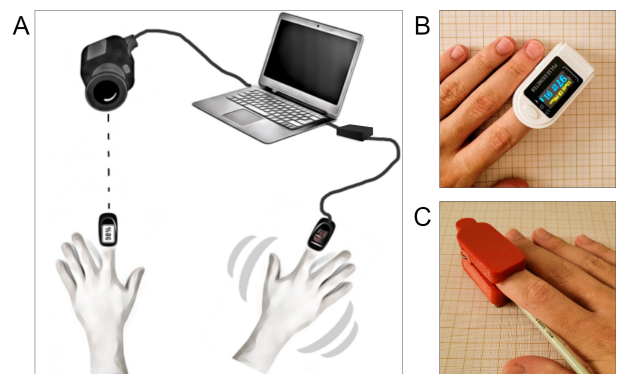
Figure 4. Method used to obtain the oximetric parameters. (A) A camera was used to capture the standard-parameters (left hand) to synchronize with the values obtained from oximeter under development (right hand). (B) Pulse oximeter Model L5. (C) Fingertip-clip of pulse oximeter under development.
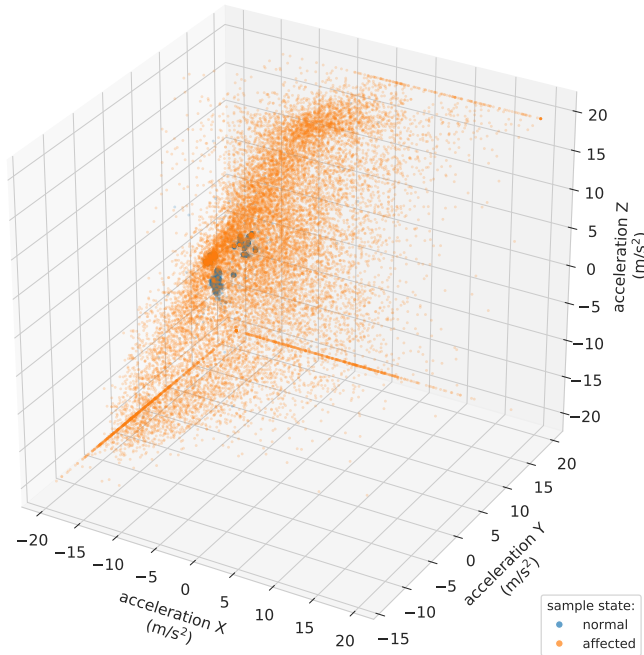
Figure 5. Oximeter 3-axis acceleration versus motion artifact.

2.2 Exploratory Data Analysis

After the collections were completed, a pre-processing of the data was carried out in order to understand how the data were distributed, facilitating its visualization and interpretation. Thus, it is very important that the data are understood and properly processed. Visualization techniques are very useful to show, in a summarized way, important characteristics of the data. This step was essential to understand the problem and seek the most appropriate technique to deal with motion artifact.

To analyze the relationship between the variables of the created dataset, scatter plots were created to analyze the influence of movement on PPG signals. In Figure 5, it is possible to see the distribution of samples classified as *normal* and *affected* by motion artifacts. Figure 6 show that the amplitude of the movement (observed by the amplitude of the acceleration dispersion) is the major factor for the sample to be classified as affected, as expected.

Boxplots were also created to facilitate the visualization of the distribution of each attribute, as well as to analyze the presence of outliers. Figure 7 presents the boxplots for each class of the problem, i.e., for the samples that remained normal (A) and for those that were affected (B) and, consequently, produced erroneous SpO_2 and HR estimations.

As expected, the samples belonging to the *affected* class presented a greater degree of dispersion in the data of each attribute. Except for the *PPG IR* and *PPG Red* attributes which maintained a more similar interquartile range in both rest and motion states. This once again confirms that acceleration is the preponderant factor to characterize the sample as *affected* or *normal*. During the manual process of labeling the data, i.e., identifying the class of each sample, certain samples were classified as *normal* although they belonged to the class of *affected* and therefore it is possible
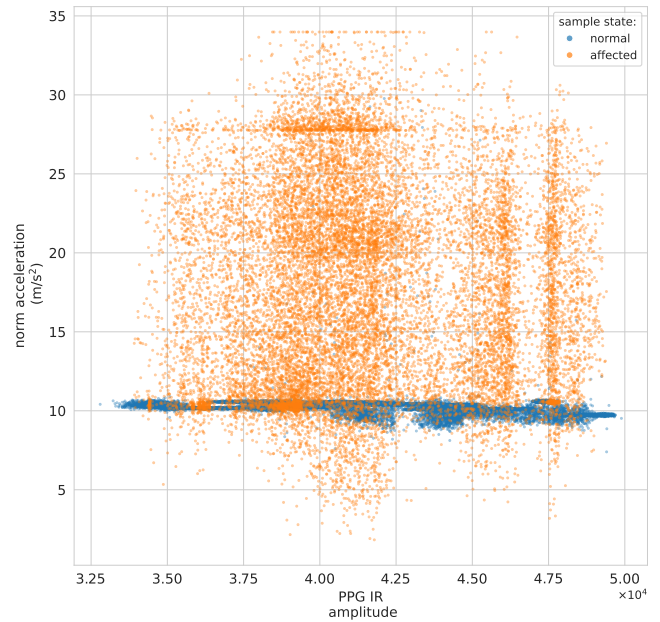
Figure 6. Oximeter norm acceleration and PPG infrared. Herein, it is possible to notice that the bulk of the samples belonging to the *normal* class remain intact throughout steady state, around 10 m/s².

to see the presence of these outliers in the acceleration boxplots during rest. This issue did not affect the ANN training, as there were few samples and no problems were observed in the debugging process.
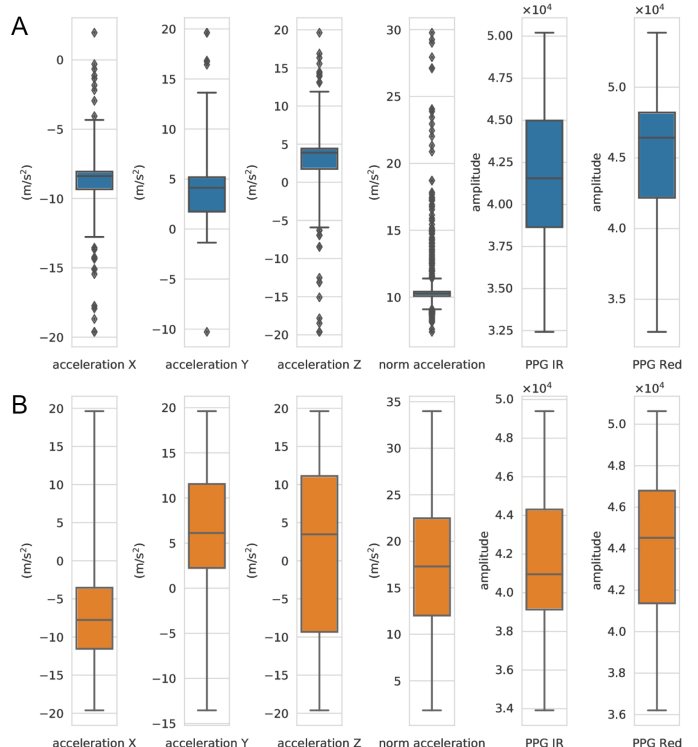
Figure 7. Boxplots for the samples that remained *normal* (A) and those that were *affected* (B) by motion artifact. In the *normal* class it is possible to see some outliers in the acceleration attributes coming from the data labeling process.

2.3 Multilayer Perceptron

From the created dataset, ANNs based on MLP were implemented to identify the samples in which the PPG signals were affected and it was not possible to observe their characteristic waveform. Figure 8 shows the samples of PPG signals that were affected (1) and those that remained normal (0) during the acquisition.
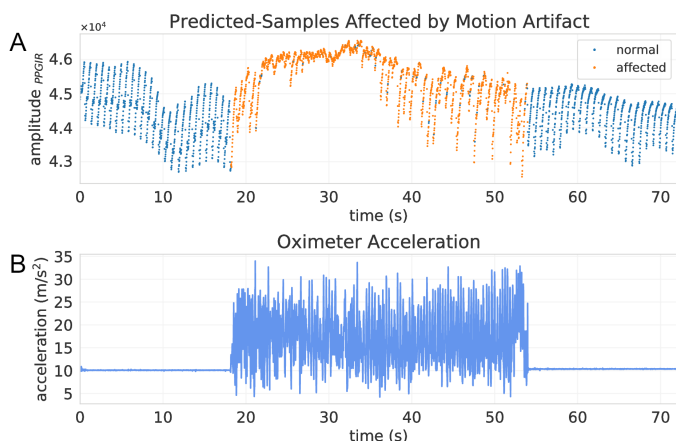
Figure 8. Samples predicted by the ANN as *normal* and *affected* by motion artifact in one of the collects. (A) Representation of predictions made by the sample classifier. (B) Range where the oximeter moves.

The Backpropagation algorithm was used to train the ANNs. Of the 40 collections performed, 30 were used for training and 10 were used to analyze the performance of the evaluated models. Eleven tests were performed with different topologies of ANNs in order to evaluate each model as a function of the number of input attributes, number of neurons and performance of the networks. Figure 9 summarizes the average performance and the standard deviation of the results predicted by each model for the 10 test collections. These results were properly discussed in section 4.

3. ALGORITHM IMPLEMENTATION

The algorithm named OxiTidy v.1 proposed in this paper aims to mitigate measurement errors and false alarms in SpO_2 and HR estimations using an IMU. It works mainly in cases where the PPG signals are affected by noise caused by the users movements. For this, it has a 3-axis accelerometer and a savgol-filter of polynomial order equal to 3 and window width of 7 (samples). The procedure for the OxiTidy v.1 algorithm is presented in Table 1.

According to Yan et al. (2005), the rate of change of oxime-try measurements is relatively slow, therefore, SpO_2 that changes by more than 2% per second can be considered to be physiologically impossible, which could indicate a false alarm. Based on this premise, OxiTidy v.1 detects samples affected by MA and disregards these measurements, which are replaced by interpolated values from two known normal estimations. In other words, instead of displaying the incorrect value, it shows a more accurate value, given the established range.

Table 1. OxiTidy v.1 algorithm: SpO_2 and HR estimations.

Stage 1	Raw data acquisition
1.1	Gets PPG IR and Red signals, and 3-axis acceleration (xyz).
Stage 2	**Sample state prediction using ANN (MLP 3-3-1)**
2.1	Gets 3-axis acceleration to predict sample state (affected or normal).
Stage 3	**Savitzky-Golay filter**
3.1	Apply savgol-filter on PPG IR and Red signals.
Stage 4	**Calculation of AC and DC components every 6 seconds**
4.1	Uses all samples collected within a 6-second period to calculate AC and DC for PPG IR and Red signals.
Stage 5	**SpO_2 estimation**
5.1	Computes R ratio (eq. 1) using values of substage 4.1.
5.2	Estimates SpO_2 (eq. 2) using value of substage 5.1.
Stage 6	**HR estimation**
6.1	Uses PPG IR signal to calculate 1st derivative (within a 6-second period).
6.2	Gets the absolute values of substage 6.1.
6.3	Finds the peaks referring to the cardiac cycle.
6.4	Computes the number of peaks found in substage 6.3 to estimate HR in bpm.
Stage 7	**Removal of affected samples**
7.1	If the number of affected samples is greater than 1% (within a 6-second period), the calculated SpO_2 is rejected (NaN).
7.2	If the number of affected samples is greater than 1% (within a 6-second period), the calculated HR is rejected (NaN).
Stage 8	**Correction of NaN[1] values**
8.1	For each standard 6-second period, interpolates the NaN values using two regular SpO_2 measurements.
8.2	For each standard 6-second period, interpolates the NaN values using two regular HR measurements.

[1] NaN standing for *Not a Number*, is a symbol used to represent an undefined numeric value.

In this algorithm, SpO_2 and HR measurements were estimated in a 6-second window, i.e., at each 6-second section a new measurement of each parameter was computed from the samples corresponding to that section. To guarantee that at least two positive and two negative pulse peaks were present in any given window, the window width was set to 6 seconds (Johnston, 2006).

As it was found, and it was expected, the ANN prediction process presented a small error where samples that belonged to the *affected* class were classified as *normal* and vice versa. This can be seen in Figure 8 (A). For this, in the algorithm proposed here, a threshold was implemented precisely to make this distinction between the two classes. During the tests with the data predicted by the ANN, the threshold of 1% of samples affected was reached, i.e., if the number of samples affected in a section was greater than 1%, these measurements were rejected and, in this referred section, SpO_2 and HR estimations were linearly interpolated from two measurements obtained with samples from a section with a threshold less than or equal to 1%.

4. RESULTS AND DISCUSSION

The first step, based on exploratory data analysis, was to define an appropriate technique capable of classifying samples affected by MA. In order to identify the intervals where the PPG signals were affected by the MA, different topologies of ANNs based on the MLP were evaluated.

The performance metrics used to evaluate each ANN were summarized in Figure 9 below. It is possible to observe that the acceleration was the major factor to determine the state of the sample, and the use of an accelerometer was fundamental since the information coming only from the PPG signals were not enough for the ANNs to achieve a good performance.
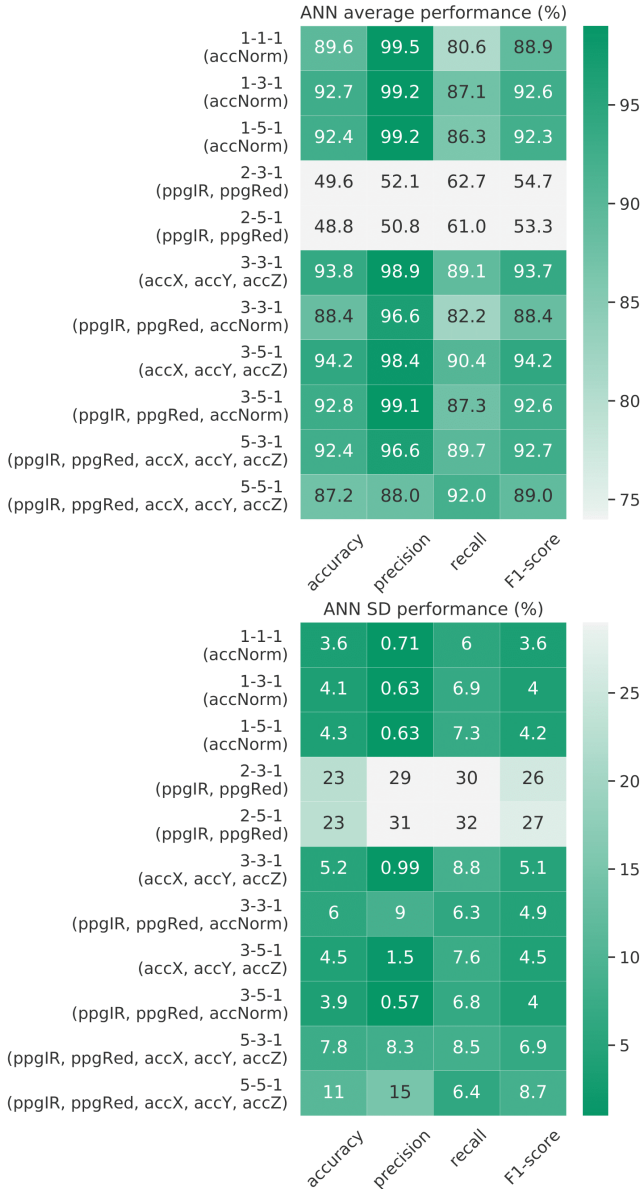
Figure 9. Performance of the ANNs evaluated. Herein, it is possible to verify the *average performance* and *standard deviation* of each ANN. Again it is possible to see that acceleration (acc) is the preponderant factor in the sample classification process.

Aiming at a good performance in the face of the four evaluated metrics and a simplified ANN topology, the 3-3-1 model was chosen, applying the acceleration attributes in the xyz-axes to the ANN input. Table 2 shows the details of the ANN used in OxiTidy v.1.

To evaluate the performance between the two approaches presented in this paper, the SpO_2 *bias* and *precision*, and

Table 2. MLP neural network parameters.

Parameter/method	Value/description
No. of hidden layers	1
No. of hidden neurons	3
No. of output neurons	1
Learning algorithm	Backpropagation
Activation function of hidden neurons	Hyperbolic tangent
Activation function of output neurons	Sigmoid
Learning epochs	20
Input data preprocessing	StandardScaler (sklearn)

the *mean absolute error* (MAE) were calculated (Barker, 2002). The *bias* and *precision* are defined as the mean and standard deviation of the differences between the SpO_2 reference values (measured by a certified oximeter) and the values estimated by the proposed algorithm, respectively. These error measures were used to evaluate the estimations without any processing (*raw*) and those performed by *OxiTidy v.1* while the subject was in a position of rest and motion. These results are summarized in Table 3 below.

Table 3. Performance statistics of the two approaches.

State	Approach	SpO_2 bias (%)	SpO_2 precision (%)	HR MAE (bpm)
resting	raw	3.22	2.23	6.28
	OxiTidy v.1	1.46	1.03	2.86
motion	raw	4.09	3.32	13.08
	OxiTidy v.1	1.51	0.92	4.18

Note that the OxiTidy v.1 approach demonstrates a significant improvement in both SpO_2 and HR estimations when compared to the approach where there is no signal processing. This was observed both in the resting state and during motion. It is evident that the savgol-filter fulfilled its role in the presence of MAs and, especially, in the intervals where the oximeter remained at rest. The ANN also performed well in the intervals where there was movements, keeping the metrics similar during rest and motion for the evaluated dataset.

It should be considered that these results are limited to a dataset of a single subject with normal oxygen saturation. Therefore, the next step would be to evaluate the performance of the algorithm proposed here in low saturation conditions and in a larger group of people. OxiTidy could also be compared with other techniques such as FFT, weighted moving average (WMA), etc. Thus, it would be possible to assess the performance of this algorithm with the other techniques present in the literature.

Indeed, OxiTidy v.1 is applied to post-processed data, i.e., the PPGs signals are collected and then the SpO_2 and HR measurements are computed. This initial version is intended to demonstrate its performance and serve as a basis for future implementations. For example, embedding it in a microcontroller to run online. For this, it would be interesting to alert the user (e.g. using a buzzer or LED) the presence of MA, thus asking the user to rest so that the measurements are correctly computed or interpolated.

5. CONCLUSION

Pulse oximetry is a non-invasive technique that allows the monitoring of physiological signals in a very simplified way. What was possible to do only with high-cost and unwieldy biomedical equipment, has been popularized with the emergence of wearable technologies. However, the way these devices are built and used directly influences the quality of the information provided to the user. There are several factors that can impair the accuracy of the data generated by the oximeters, among them is the MA. This can cause errors in the readings and cause false alarms. In order to mitigate these undesirable effects, in this paper, an algorithm based on ANN capable of detecting noise in the oximetry signal was proposed.

In this study, OxiTidy v.1 was presented to minimize the effects of movements on PPG signals to improve the accuracy of SpO_2 and HR estimations of a Wi-Fi pulse oximeter under development by the Department of Electrical Engineering, Computing Department and Medicine Department at the Federal University of São Carlos (UFSCar). The applied technique used MLP to identify the intervals where the measurements performed were incorrect and then estimated new values with a good approximation to the readings performed by an Anvisa-certified pulse oximeter. A significant improvement in SpO_2 and HR estimations was demonstrated both at rest and in motion in a limited dataset obtained from the author* of this work.

ACKNOWLEDGMENTS

REFERENCES

Barker, S.J. (2002). "Motion-Resistant" pulse oximetry: A comparison of new and old models. *Anesth. Analg.*, 95(4), 967–972.

Chacon, P.J., Pu, L., da Costa, T.H., Shin, Y.H., Ghomian, T., Shamkhalichenar, H., Wu, H.C., Irving, B.A., and Choi, J.W. (2019). A wearable pulse oximeter with wireless communication and motion artifact tailoring for continuous use. *IEEE Trans. on Biomed. Eng.*, 66(6), 1505–1513.

Cho, J.H., Kim, J.C., and Yoon, G.W. (2014). Robust design of pulse oximeter using dynamic control and motion artifact detection algorithms. *Journal of Electrical Engineering and Technology*, 9(5), 1780–1787.

ElectroPeak Inc. (2021). MPU9250 SPI/I2C 9-axis gyro accelerator magnetometer module. URL `bit.ly/3zlSMND`.

Gallagher, N.B. (2020). Savitzky-Golay smoothing and differentiation filter. *Eigenvector Research Incorporated.*

Giuliano, K.K. and Liu, L.M. (2006). Knowledge of pulse oximetry among critical care nurses. *Dimens. Crit. Care Nurs.*, 25(1), 44–49.

Haghi, M., Thurow, K., and Stoll, R. (2017). Wearable devices in medical internet of things: Scientific research and commercially available devices. *Healthcare Informatics Research*, 23(1), 4–15.

Hayes, M.J. and Smith, P.R. (2001). A new method for pulse oximetry possessing inherent insensitivity to artifact. *IEEE Trans. on Biom. Eng.*, 48(4), 452–461.

InvenSense Inc. (2014). MPU-9250 product specification - revision 1.0. URL `bit.ly/3SvRgRV`.

Johns Hopkins Medicine (2022). Vital signs (body temperature, pulse rate, respiration rate, blood pressure). URL `bit.ly/3BtwjAS`.

Johnston, W.S. (2006). *Development of a Signal Processing Library for Extraction of SpO2, HR, HRV, and RR from Photoplethysmographic Waveforms.* Master's thesis, Worcester Polytechnic Institute.

Lee, J., Jung, W., and Kang, I. (2003). Design of filter to reject motion artifact of pulse oximetry. *Computer Standards & Interface*, 26, 241–249.

Maxim Integrated (2018). Recommended configurations and operating profiles for MAX30101/MAX30102 EV kits. URL `bit.ly/3Qcaw4N`.

Mendelson, Y. (1992). Pulse oximetry: theory and applications for noninvasive monitoring. *Clinical Chemistry*, 38(9), 1601–1607.

Press, W.H. and Teukolsky, S.A. (1990). Savitzky-Golay smoothing filters. *Comput. Phys. Commun.*, 4(6), 669.

Rodrigues, E.M., Godina, R., Cabrita, C.M., and Catalão, J.P. (2017). Experimental low cost reflective type oximeter for wearable health systems. *Biomedical Signal Processing and Control*, 31(1), 419–433.

Salehizadeh, S.M.A., Dao, D.K., Chong, J.W., McManus, D., Darling, C., Mendelson, Y., and Chon, K.H. (2014). Photoplethysmograph signal reconstruction based on a novel motion artifact detection-reduction approach. part ii: Motion and noise artifact removal. *Annals of biomedical engineering*, 42(11), 2251–2263.

Savitzky, A. and Golay, M.J.E. (1964). Smoothing and differentiation of data by simplified least squares procedures. *Analytical Chemistry*, 36(8), 1627–1639.

Sinchai, S., Kainan, P., Wardkein, P., and Koseeyaporn, J. (2018). A photoplethysmographic signal isolated from an additive motion artifact by frequency translation. *IEEE Trans. on Biom. Circ. and Syst.*, 12(4), 904–917.

Tarvirdizadeh, B., Golgouneh, A., Tajdari, F., and Khodabakhshi, E. (2020). A novel online method for identifying motion artifact and photoplethysmography signal reconstruction using artificial neural networks and adaptive neuro-fuzzy inference system. *Neural Computing & Applications*, 32(8), 3549–3566.

Urpalainen, K. (2011). *Development of a fractional multi-wavelength pulse oximetry algorithm.* Master's thesis, Aalto University.

World Health Organization (2011). Pulse oximetry training manual. URL `bit.ly/3JkV5Fe`.

Yan, Y.S., Poon, C.C., and Zhang, Y.T. (2005). Reduction of motion artifact in pulse oximetry by smoothed pseudo wigner-ville distribution. *Journal of NeuroEngineering and Rehabilitation*, 2(1), 1–9.

Yousefi, R., Nourani, M., Ostadabbas, S., and Panahi, I. (2014). A motion-tolerant adaptive algorithm for wearable photoplethysmographic biosensors. *IEEE Journal of Biomedical and Health Informatics*, 18(2), 670–681.